Research Article

Combined treatment with valproic acid and estrogen has neuroprotective effects in ovariectomized mice with Alzheimer's disease

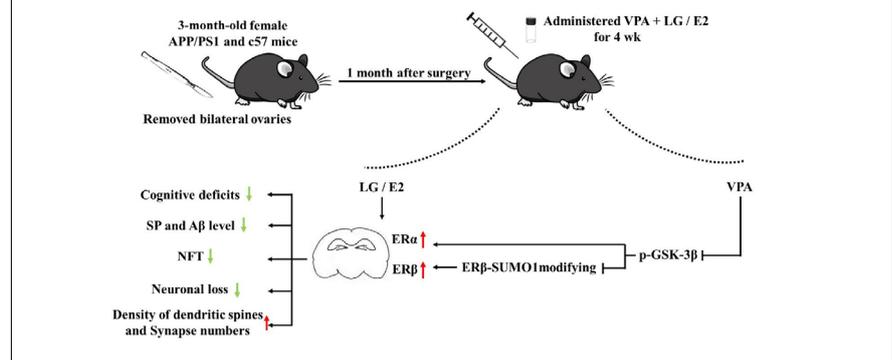Yan-Zhen Li[1, #], Yuan-Jie Liu[1, 2, #], Wei Zhang[1], Shi-Fang Luo[1, 2], Xin Zhou[3, *], Gui-Qiong He[1, 2, *]

Graphical Abstract *Valproic acid (VPA) combined with estrogen treatment is better than VPA or estrogen intervention alone in menopausal Alzheimer's disease mouse models*

Abstract

Postmenopausal women with Alzheimer's disease (AD) exhibit dramatically reduced sensitivity to estrogen replacement therapy, which is though to be related to an estrogen receptor (ER)α/ERβ ratio imbalance arising from a significantly decreased level of ERs of the brain. The aim of our study was to investigate whether valproic acid (VPA) can enhance the beneficial effects of estrogen on cognitive function through restoration of ERα and ERβ expression in the brain. We removed the ovaries of female APP/PS1 mice to simulate the low estrogen levels present in postmenopausal women and then administered VPA (30 mg/kg, intraperitoneal injection, once daily), 17β-estradiol (E2) (2.4 μg, intraperitoneal injection, once daily), liquiritigenin (LG) (50 μg/kg, intragastric infusion, once daily), VPA + E2, or VPA + LG for 4 successive weeks. Compared with treatment with a single drug, treatment with VPA + E2 or VPA + LG significantly increased the level of glycogen synthase kinase 3β, increased the expression of estrogen receptor α, reduced the expression of small ubiquitin-like modifiers, and increased the level of estrogen receptor β. This resulted in enhanced sensitivity to estrogen therapy, reduced amyloid β aggregation, reduced abnormal phosphorylation of the tau protein, reduced neuronal loss, increased dendritic spine and postsynaptic density, and significantly alleviated memory loss and learning impairment in mice. This study was approved by the Chongqing Medical University Animal Protection and Ethics Committee, China on March 6, 2013.

Key Words: 17β-estradiol; amyloid β; dementia; estrogen receptor α; estrogen receptor β; glycogen synthase kinase-3β; liquiritigenin; menopause; neuron loss; tau

Chinese Library Classification No. R453; R741; Q579.1+3

Introduction

Alzheimer's disease (AD) is a common form of degenerative neurological disorder resulting in memory loss and cognitive decline. Excessive deposition of extracellular senile plaques (SP), formation of intracellular neurofibrillary tangles, and loss of neurons are the predominant neuropathological features of AD (Goedert and Spillantini, 2006; Wang et al., 2020). Overexpression of glycogen synthase kinase 3β (GSK-3β) in patients with AD may promote amyloid β (Aβ) production, tau hyperphosphorylation, and neuronal degeneration (Hernández et al., 2010).

Valproic acid (VPA), a multifunctional drug used to treat epilepsy and bipolar disorder (Kostrouchová et al., 2007), plays important roles in promoting the release of neurotrophic factor and inducing neurogenesis (Qing et al., 2008; Hu et al., 2011). In addition, a recent study demonstrated that VPA inhibits GSK-3β activity by increasing p-Ser9-GSK-3β levels (Azab et al., 2017). Furthermore, we previously showed that

[1]Chongqing Key Laboratory of Neurobiology, Chongqing Medical University, Chongqing, China; [2]Department of Anatomy, Chongqing Medical University, Chongqing, China; [3]Department of Galactophore, Chongqing University Cancer Hospital, Chongqing, China
*Correspondence to: Xin Zhou, PhD, zhouxin75324@163.com; Gui-Qiong He, PhD, guiqionghe@cqmu.edu.cn.
https://orcid.org/0000-0002-7077-2001 (Gui-Qiong He)
#Both authors contribute equally to this work.

VPA can reduce Aβ generation, decrease tau phosphorylation, and improve memory deficits, which is consistent with other studies (Qing et al., 2008; Hu et al., 2011; Xuan et al., 2015).

An epidemiological study indicated that AD affects postmenopausal women about 1.5–3 times more often than similarly aged men, suggesting that there is a link between menopausal estrogen loss and development of the disease (Gillies and McArthur, 2010). Clinical trials have reported that estrogen replacement therapy can effectively delay and reduce the risk of AD in women prior to or in the early stages of menopause, whereas postmenopausal women with AD have a dramatically reduced sensitivity to estrogen replacement therapy (Gleason et al., 2015; Kantarci et al., 2016).The mechanism underlying this phenomenon may be related to an imbalance in the estrogen receptor (ER)α/ERβ ratio owing to significantly lower expression of ERs in the brain (Sinopoli et al., 2006). Recent research has highlighted that GSK-3β may affect ERα phosphorylation and activity (Medunjanin et al., 2005; Fortunati et al., 2010). In addition, it can regulate ERβ expression and activity through the addition of small ubiquitin-like modifier (SUMO) proteins to this receptor (Picard et al., 2012).

In the brain, ERα is mainly expressed in the hippocampus, preoptic region, and hypothalamus. ERβ is mainly expressed in the olfactory bulb, cerebral cortex, and cerebral septum. Both ERα and ERβ play indispensable roles in the formation of learning and memory (Foster, 2012). ERα and ERβ nonselectively bind estrogens, including estrone, 17β-estradiol (E2), and estriol, of which E2 has the strongest estrogenic activity. Phytoestrogens, whose structure and function are similar to those of estrogens, are effective ERβ agonists and exhibit minor toxic side effects. The phytoestrogen liquiritigenin (LG) is a highly selective ERβ agonist that has neuroprotective and neurotrophic effects (Mersereau et al., 2008).

Thus, given the evidence presented above, the aim of our study was to determine whether E2 or LG combined with VPA can ameliorate the cognitive impairment and neurodegenerative pathology observed in postmenopausal ovariectomized (OVX) APPswe/PSEN1dE9 double-transgenic (APP/PS1) mice through restoration of ERα and ERβ expression in the brain.

Materials and Methods

Animals
Eighty 3-month-old female APP/PS1 AD mice (weighing 23–27 g, specific pathogen-free) were obtained from the Biomedical Research Institute of Nanjing University (Nanjing, China; certificate No. 201800973). The animals' ovaries were removed under anesthesia to simulate the physiological state of low estrogen levels in postmenopausal women. One month after surgery (at which time the mice were 4 months old, which is equivalent to 2 to 4 years after menopause in women), the mice were randomly divided into six groups with eight mice in each group: the single-drug groups (VPA, E2, or LG), the combined treatment groups (VPA + E2 or VPA + LG), and the control group. The mice received VPA (Sigma, St. Louis, MO, USA, 30 mg/kg per day, intraperitoneal injection, once daily), E2 (Sigma, 2.4 μg per mouse, once a day, intraperitoneal injection), LG (Shanghai Macklin Biochemical Co., Ltd., Shanghai, China, 50 μg/kg per day, intragastric infusion, once a day), or 0.9% sodium chloride (0.25 mL) for 4 weeks. All experiments were approved by the Chongqing Medical University Animal Protection and Ethics Committee on March 6, 2013. The mice were housed in cages in a laminar flow rack exposed to a 12 hours on/12 hours off light cycle and were given free access standard rodent chow and water, within a temperature-controlled room (20–25°C).

Morris water maze
The Morris water maze (MWM) apparatus (SLY-WMS 2.0; Shanghai Bio-will Co., Ltd., Shanghai, China) consisted of a circular tank 120 cm in diameter and 47 cm deep. The tank contained warm water that was maintained at 25 ± 0.5°C and was divided into four quadrants that were marked with cues on the exterior. A transparent escape platform (10 cm in diameter) was set 1 cm above the water level on day 1. Each mouse was allowed to freely explore the platform for 60 seconds. If the animal failed to locate the platform within 60 seconds, the mouse would be placed on it for 15 seconds. The hidden platform test consisted of four consecutive training days. The platform was submerged to a depth of 1 cm under the surface of the water. Spatial learning and memory were assessed by measuring escape latency and path length to reach the hidden platform in 60 seconds. During the probe test, the platform was removed from the pool, and the mice were allowed to swim freely for 60 seconds. All paths from all trials were analyzed using water maze software (Lyu et al., 2020).

Immunofluorescence and thioflavin S staining
Animals were euthanized by CO_2 inhalation after the behavioral experiments were complete. Next, the brains were removed, and half of each brain was dehydrated for 24 hours in a series of sucrose solutions (10%, 20%, and 30%), after which they were fixed in 4% paraformaldehyde overnight. These brain samples were then cut into 10-μm-thick coronal sections and used for immunofluorescence staining and thioflavin S staining (0.1%; Zhuhai Fei Yang Novel Materials Co., Ltd., Zhuhai, China). Immunofluorescence staining was performed by treating with 3% hydrogen peroxide and blocking in 10% fetal calf serum. The slides were incubated with a mouse anti-Aβ monoclonal 4G8 antibody (1:250; Cat# SIG-39240; Covance, Princeton, NJ, USA) at 4°C overnight. Subsequently, the slides were incubated with a goat anti-mouse IgG (H+L) CY3-conjugated secondary antibody (1:300; Affinity Biosciences, Changzhou, China) at 37°C for 1 hour, followed by a DAPI solution (Solarbio, Beijing, China). For thioflavin S staining, after being subjected to an ethanol gradient and 0.1% $KMnO_4$ treatment, sections were incubated with thioflavin S (0.1% in 80% of ethanol) for 8 minutes at room temperature, washed with ethanol (80% and 70% each for 30 seconds), and rinsed with distilled water twice. The slides were mounted with aqueous mounting media and dried in the dark overnight. Finally, all of the sections were visualized, and images were captured, using a digital fluorescence microscope (Leica Microsystems, Wetzlar, Germany), and the mean number of plaques per slice in the cortex and hippocampus of the six groups was quantified.

Enzyme-linked immunosorbent assay
The other half of each brain from each mouse was analyzed for $A\beta_{40}$ and $A\beta_{42}$ expression levels using an $A\beta_{1-40}$ and $A\beta_{1-42}$ Assay Kit (IBL, Minneapolis, MN, USA) according to the manufacturer's instructions. The Aβ concentration in the brain tissues was calculated from standard curves.

Western blot analysis
Total protein was extracted from the collected mouse brain tissues using cold lysis buffer containing a protease inhibitor. The protein concentrations were determined by the bicinchonininc acid method (Beyotime Biotechnology, Shanghai, China). Equal amounts of protein from different samples were separated on sodium dodecyl sulfate-polyacrylamide gel electrophoresis gels and then electrotransferred onto a 0.45-μm polyvinylidene fluoride membrane (Millipore, Burlington, MA, USA). After the membrane was immersed in 3% bovine serum albumin for 2 hours, target proteins were detected using primary antibodies to amyloid precursor protein (APP; Cat# ab241592; 1:1000; Abcam, Cambridge, MA, USA), β-amyloid precursor protein cleavage enzyme-1 (BACE1; Cat# ab2077; 1:1000; Abcam), presenilin-1 (PS1; Cat# ab76083; 1:1000; Abcam), insulin-

degrading enzyme (IDE; Cat# ab133561; 1:1000; Abcam), neprilysin (NEP; Cat# ab58968; 1:1000; Abcam), tau-5 (Cat# ab80579; 1:1000; Abcam), paired helical filament-1 (PHF-1; Cat# ab184951; 1:1000; Abcam), neuronal nuclei antigen (NeuN; Cat# 24307; 1:1000; CST, Danvers, MA, USA), growth associated protein-43 (GAP43; Cat# ab75810; 1:1000; Abcam), postsynaptic density-95 (PSD-95; Cat# ab76115; 1:1000; Abcam), ERα (Cat# ab32063; 1:800; Abcam), ERβ (Cat# ab3577; 1:1000; Abcam), GSK-3β (Cat# ab93926; 1:1000; Abcam), p-GSK-3β (Ser9) (Cat# b75814; 1:500; Abcam), small ubiquitin-like modifier 1 (SUMO1; Cat# sc-5308; 1:500; Santa Cruz Biotechnology, Santa Cruz, CA, USA), and β-actin (Cat# A5441; 1:1000; Sigma). The membranes were then incubated with goat anti-rabbit IgG (H+L) horseradish peroxidase (1:5000, Cat# S0001, Affinity Biosciences, Cincinnati, OH, USA) or goat anti-mouse IgG (H+L) horseradish peroxidase (1:5000, AS003, ABClonal, Wuhan, China) at 37°C for 40 minutes. Immunoreactive bands on the membrane were visualized by enhanced chemiluminescent detection (Beyotime Biotechnology). Relative expression was determined using Image Lab software (Bio-Rad, Hercules, CA, USA).

Golgi staining

Dendritic spine structure was observed by Golgi staining (He et al., 2020) using the FD Rapid Golgi Stain Kit (FD Neurotechnology, Inc., Columbia, MD, USA). All procedures were conducted in the dark. The brain tissues were immersed in a mixture of equal volumes of solutions A and B at room temperature for 2 weeks, after which the tissues were transferred to solution C for 72 hours. Next, 100-μm thick coronal sections were cut using a cryostat microtome at –22°C, and mounted on gelatin-coated microscope slides using solution C. A staining solution (one part solution D, one part solution E, and two parts DW) was used to stain the sections for 5 minutes. After the sections were dehydrated and cleared, coverslips were applied using neutral gum (Biosharp, Guangzhou, China). Golgi-stained sections were analyzed with an optical microscope (DFC425 C; Leica).

Transmission electron microscopy

One millimeter-thick sections were cut from the cortex and from hippocampal region CA1 of the mouse brains. The specimens were fixed in 3% glutaraldehyde for 2 hours, followed by 1% osmium tetroxide for 2 hours, and then dehydrated with a graded acetone series. Next, the tissues were embedded in epoxy resin and sliced into 100-nm-thick sections. Finally, the ultrathin sections were stained with uranyl acetate and lead citrate, and the synaptic ultrastructural changes were captured and observed with a transmission electron microscope (Philips, Amsterdam, The Netherlands).

Statistical analysis

Data are presented as the mean ± error of the mean (SEM). All quantitative results were analyzed using Graph Pad Prism 6 software (GraphPad Software Inc., La Jolla, CA, USA). The MWM data were analyzed by two-way analysis of variance with Student-Newman-Keuls tests. For all other data, one-way analysis of variance was used, followed by Tukey's *post hoc* test. In all cases, a *P*-value < 0.05 was considered statistically significant.

Results

VPA combined with estrogen ameliorates memory and learning deficits in OVX AD mice

To test whether treatment with VPA and estrogen improves spatial memory and learning in OVX AD mice, an MWM test was conducted after 4 weeks of treatment. No statistically significant differences were found in escape latency (*F* = 0.4247, *P* = 0.8255) or path length (*F* = 1.684, *P* = 0.1895) for the visible platform test among all groups (**Figure 1A** and **B**), which indicated that the treatment regimen did not affect vision or motility. For the hidden platform task, the combination treatment groups exhibited a considerable decrease in escape latency (*F* = 2.167, *P* = 0.0091) and path length (*F* = 1.165, *P* = 0.3029) compared with the single-drug groups and the control group (**Tables 1** and **2**). In the probe trials, the mice in the combination treatment groups traveled across the platform zone more often than those in the control group and single-drug groups. Furthermore, the VPA + LG group exhibited superior performance in the probe trial compared with the VPA + E2 group (*F* = 19.38, *P* < 0.0001; **Figure 1C**). These data indicated that the spatial memory and learning of OVX AD mice was improved after treatment, and that treatment with VPA and estrogen was more effective than treatment with VPA, E2, or LG alone.

VPA combined with estrogen decreases SPs and Aβ expression levels in the brain in OVX AD mice

Impairments in memory and cognitive functions are closely related to increased levels of Aβ (Selkoe and Hardy, 2016).

Table 1 | Hidden platform test escape latency (in seconds) in an ovariectomized mouse model of Alzheimer's disease

Group	Day 1	Day 2	Day 3	Day 4	Day 5
Control	58.89±0.78	56.20±1.87	51.04±0.84	46.98±1.99	42.08±2.71
VPA	56.37±1.66	50.17±1.03	46.30±0.94	41.06±0.62	37.20±2.78
E2	57.28±0.95	44.76±1.56[****]	42.95±1.37[**]	39.66±1.17[*]	37.26±1.21
LG	52.66±0.97	44.80±1.22[****]	44.94±0.56	37.33±1.34[***]	32.18±1.97[***]
VPA+E2	52.17±1.28[*]	44.35±0.84[****]	37.55±1.50[****]	30.01±1.68[****]	25.60±1.51[****]
VPA+LG	47.10±1.36[****]	38.96±1.69[****]	32.65±2.04[****]	26.20±0.93[****]	19.67±2.87[****]

Data are presented as the mean ± SEM (*n* = 8). *P < 0.05, **P < 0.01, ***P < 0.001, ****P < 0.0001, *vs.* control group (two-way analysis of variance with Student-Newman-Keuls tests). E2: 17β-Estradiol; LG: liquiritigenin; VPA: valproic acid.

Table 2 | Hidden platform test change in path length (in m) in an ovariectomized mouse model of Alzheimer's disease

Group	Day 1	Day 2	Day 3	Day 4	Day 5
Control	7.77±1.09	6.14±0.31	5.97±0.33	5.89±0.44	5.59±0.26
VPA	7.01±0.78	5.75±0.26	4.98±0.27	3.33±0.22[**]	3.75±0.28
E2	5.33±1.01[**]	3.67±0.34[**]	3.24±0.40[**]	2.10±0.34[****]	2.13±0.42[****]
LG	6.88±0.98	5.82±0.13	4.59±0.43	3.51±0.51[**]	2.70±0.19[***]
VPA+E2	5.76±0.36[*]	4.85±0.26	3.35±0.43[**]	2.69±0.12[****]	2.14±0.10[****]
VPA+LG	6.67±0.29	4.22±0.41[*]	2.90±0.31[***]	2.04±0.35[****]	1.66±0.25[****]

Data are presented as the mean ± SEM (*n* = 8). *P < 0.05, **P < 0.01, ***P < 0.001, ****P < 0.0001, *vs.* control group (two-way analysis of variance with Student-Newman-Keuls tests). E2: 17β-Estradiol; LG: liquiritigenin; VPA: valproic acid.

To examine whether the combined treatment with VPA and estrogen alters APP processing and inhibits Aβ production, SPs were detected in OVX AD mouse brains. Immunostaining showed SP immunopositivity in the hippocampus and cortex of all of the treated groups (except for the group treated with E2 only) that was significantly reduced compared with the control group. The immunopositive SPs were noticeably smaller in the VPA + LG group than those in the control group and the single-drug groups (F = 26.18, P < 0.0001; **Figure 2A** and **C**). Moreover, thioflavin S staining also showed a noticeable reduction in SP formation in the hippocampus and cortex of mice in the two combined treatment groups (F = 14.14, P < 0.0001; **Figure 2B** and **D**). However, no difference in SP formation was observed between the VPA + LG and VPA + E2 groups (P > 0.05).

To further elucidate the effects of the combination treatment on Aβ elevation, the expression levels of $Aβ_{40}$ and $Aβ_{42}$ in the hippocampus and cortex of the OVX AD mice were measured by enzyme-linked immunosorbent assay (**Figure 2E** and **F**). $Aβ_{40}$ expression was markedly decreased in the VPA + LG group compared with the control group (F = 16.74, P < 0.0001), and $Aβ_{42}$ expression was lower in all treatment groups (except for the E2 group) compared with the control group (F = 15.09, P = 0.0007). However, no difference in $Aβ_{42}$ expression was observed between the VPA + LG and VPA + E2 groups (P > 0.05). Taken together, these observations suggest that combined therapy is more affective at inhibiting Aβ production than single-drug treatment.

VPA combined with estrogen decreases Aβ formation and increases Aβ degradation in the brain in OVX AD mice
BACE1 and PS1 are the key enzymes involved in APP processing and Aβ production, while IDE and NEP are the main proteases involved in Aβ degradation (Murphy and LeVine, 2010). To further explore whether combined treatment could decrease the Aβ burden by regulating APP processing in the brains of OVX AD mice, APP, BACE1, PS1, IDE, and NEP expression were analyzed by western blot was analyzed. No detectable difference was observed in APP expression among all groups (F = 0.7375, P = 0.6096). BACE1 (F = 11.24, P = 0.0003) and PS1 (F = 15.09, P < 0.0001) expression levels were significantly lower in the combination treatment groups compared with the control group (**Figure 3A** and **C**). Furthermore, IDE expression was significantly higher in the VPA + E2 and VPA + LG groups compared with the control and single-drug groups (F = 6.393, P < 0.0004). Similarly, NEP expression was higher in the VPA-only group and in both of the combined treatment groups than in the control group (F = 41.95, P < 0.0001; **Figure 3B** and **D**). However, no difference in BACE1, PS1, or IDE expression was detected between the VPA + LG and VPA + E2 groups.

VPA combined with estrogen prevents tau hyperphosphorylation in the brain in OVX AD mice
Abnormally hyperphosphorylated tau facilitates its aggregation into PHFs, which in turn become the main constituent of the neurofibrillary tangles that are characteristic of AD (Šimić et al., 2016). We examined expression of total tau (tau-5) and phosphorylated tau (PHF-1) by western blot. No difference in tau-5 expression was observed among all of the groups (F = 1.782, P = 0.1911). In contrast, all of the drug treatment groups exhibited a significant decrease in PHF-1 levels compared with the control group (F = 111.6, P < 0.0001; **Figure 4A** and **B**). However, no significant difference in PHF-1 expression was observed between the VPA + LG and VPA + E2 groups (P > 0.05).

VPA combined with estrogen attenuates neuronal loss in the brain in OVX AD mice
Given that neuronal loss is a fundamental pathological feature of AD (Vasic et al., 2019), we next asked whether combined treatment could attenuate neuronal loss. To test this, we evaluated expression of NeuN, marker of mature neurons (Lorenz et al., 2005), by western blot. We found that NeuN was expressed at higher levels in all drug treatment groups (except for the VPA group) compared with the control group (F = 6.331, P = 0.0042; **Figure 5A** and **B**). Since dendritic spines are known to be synaptic sites on neuronal dendrites, and are closely related to learning and memory (Chidambaram et al., 2019), we used Golgi staining to detect whether treatment altered neuronal dendritic spine density. The density of the dendritic spines was increased in the LG group and the combination groups compared with the control group (F = 7.043, P < 0.0001; **Figure 5C** and **D**). However, no difference in NeuN expression or dendritic spine density was observed between the VPA + LG and VPA + E2 groups (P > 0.05).

VPA combined with estrogen modulates synaptic structure in the hippocampus in OVX AD mice
Both biochemical and morphological changes in synapses are key factors affecting learning and memory (Spires-Jones and Hyman, 2014). Therefore, we analyzed synaptic ultrastructural changes by transmission election microscope. The results showed that the number of synapses in the hippocampus was increased in the combined treatment groups compared with the control and single-drug groups (F = 9.191, P < 0.0001; **Figure 6A** and **B**). Moreover, the PSD layer was significantly thicker in all of the drug groups (except for the E2 group) than in the control group (F = 4.797, P = 0.0023; **Figure 6C**). The synaptic cleft width and synaptic active zone length were also higher in the combined treatment groups than in the control group (F = 9.442, P < 0.0001; **Figure 6D** and **E**).

Synaptic function is associated with cognition and depends on the normal integration of glutamate receptors at the PSD (de Bartolomeis et al., 2014). Thus, western blot was used to investigate GAP-43 and PSD-95 expression. GAP-43 (F = 16.17, P < 0.0001) and PSD-95 (F = 11.51, P = 0.0003) expression levels were significantly higher in the combined treatment groups compared with the control and single-drug groups (**Figure 6F** and **G**).

VPA combined with estrogen inhibits GSK-3β and improves ER sensitivity in the brain in OVX AD mice
The GSK-3β kinase is rich in serine (Ser) and threonine (Tyr), and its activity is inhibited by Ser9 phosphorylation (Azab et al., 2017). Thus, we next sought to evaluate the relationship between drug treatment and the relative levels of total GSK-3β and p-GSK-3β (Ser9). No significant differences in GSK-3β expression was found among all of the groups (F = 2.141, P = 0.1299). However, p-GSK-3β expression was significantly increased in the treatment groups, especially the combined treatment groups, compared with the control group (F = 16.32, P < 0.0001; **Figure 7A** and **B**).

ERα and ERβ are the two main subtypes of ER that are expressed in the brain (Foster, 2012). We examined ERα and ERβ expression by western blot and found that ERα expression was higher in all of the single-drug groups except for the VPA-only group, and was significantly higher in the combined treatment groups, than in the control group (F = 25.05, P < 0.0001; **Figure 7C** and **D**). Additionally, there was a significant increase in ERβ expression in all of the drug treatment groups, except the VPA-only treatment group, compared with the control group (F = 138.9, P < 0.0001; **Figure 7C** and **E**).

Finally, given that change in ER expression levels may be associated with ER SUMOylation (Picard et al., 2012), we detected SUMO1 by western blot. A significantly lower level of SUMO1 was detected in the single-drug and combined treatment groups compared with the control group (F = 28.10, P = 0.0004; **Figure 7C** and **F**).
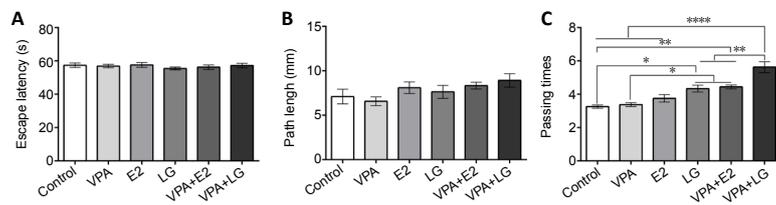
Research Article

Figure 1 | Spatial memory and learning as assessed by Morris water maze test in an ovariectomized mouse model of Alzheimer's disease after 4 weeks of drug administration.
In the visible platform test, no statistically significant differences were found in escape latency (A) and path length (B) among the six groups ($P > 0.05$). (C) In the probe trial, the mice in the combined treatment groups traveled across the platform zone more often in a 60-second period than those in the control and single-drug groups. Data are presented as the mean ± SEM ($n = 8$). *$P < 0.05$, **$P < 0.01$, ***$P < 0.001$, ****$P < 0.0001$ (two-way analysis of variance with Student-Newman-Keuls tests). E2: 17β-Estradiol; LG: liquiritigenin; VPA: valproic acid.
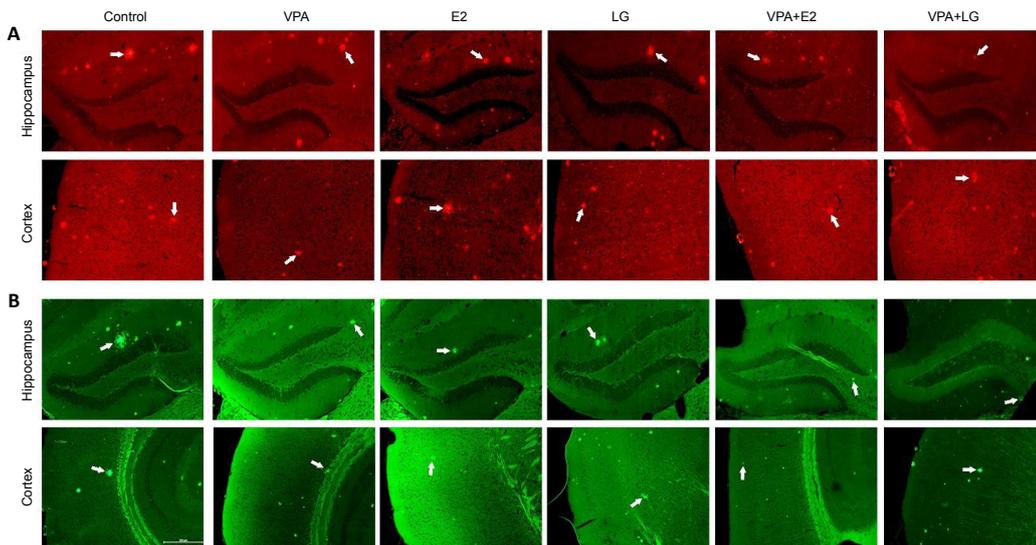
Figure 2 | Combined treatment with VPA and estrogen decreases SP formation and Aβ levels in an ovariectomized mouse model of Alzheimer's disease after 4 weeks of drug administration.
Immunohistochemistry (A) and thioflavin S staining (B) revealed SPs in the hippocampus and cortex. Scale bar: 200 μm. (A, C) There was a significant reduction in the number of SP-immunopositive spots in the hippocampus and cortex of all drug groups, except the E2 group, compared with control group. The VPA + LG group exhibited noticeably fewer SP-immunopositive spots than the control and single-drug groups. (B, D) Thioflavin S staining showed a noticeable reduction in SP formation in the hippocampus and cortex of mice in the two combined treatment groups. (E, F) Enzyme-linked immunosorbent assay results showing that Aβ$_{40}$ (E) and Aβ$_{42}$ (F) concentrations in the brain. Aβ$_{40}$ and Aβ$_{42}$ were expressed at significantly lower levels in the combined treatment group than in the control group. Data are presented as the mean ± SEM ($n = 8$). *$P < 0.05$, **$P < 0.01$, ***$P < 0.001$, ****$P < 0.0001$ (one-way analysis of variance followed by Tukey's *post hoc* test). Aβ: Amyloid β; E2: 17β-estradiol; LG: liquiritigenin; SP: senile plaques; VPA: valproic acid.
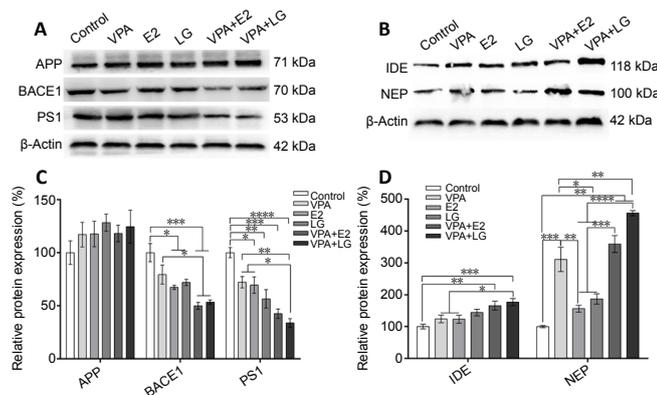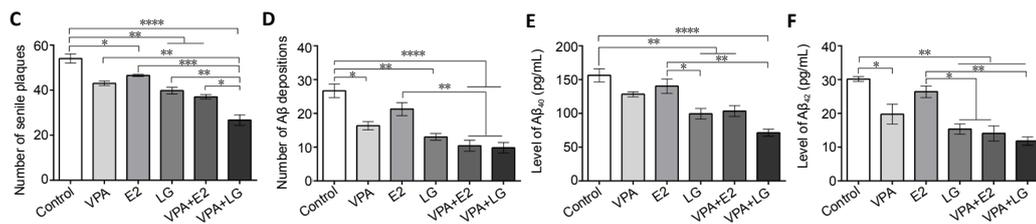

Figure 3 | Combined treatment with VPA and estrogen decreases Aβ production and increases Aβ degradation in the brain in an ovariectomized mouse model of Alzheimer's disease after 4 weeks of drug administration.
(A, B) Western blot showing APP, BACE1, PS1, IDE, and NEP expression in all groups. (C) Quantification of the significant decrease in BACE1 and PS1 expression observed in the combined treatment groups compared with the control group. No detectable difference in APP expression was observed among the groups. (D) IDE was significantly higher in the VPA + E2 and VPA + LG groups than in the control and single-drug groups. NEP expression was higher in the VPA and combined treatment groups compared with the control group. Relative protein expression was normalized to the control group. Data are presented as the mean ± SEM ($n = 8$). *$P < 0.05$, **$P < 0.01$, ***$P < 0.001$, ****$P < 0.0001$ (one-way analysis of variance followed by Tukey's *post hoc* test). APP: Amyloid precursor protein; BACE1: β-amyloid precursor protein cleavage enzyme-1; E2: 17β-estradiol; IDE: insulin-degrading enzyme; LG: liquiritigenin; NEP: neprilysin; PS1: presenilin-1; VPA: valproic acid.
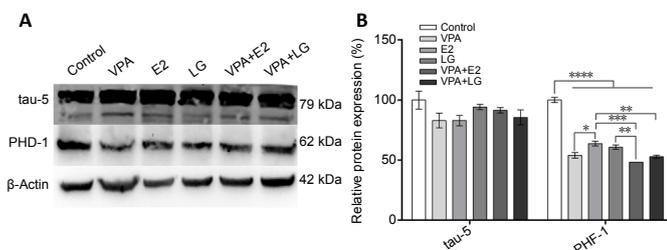

Figure 4 | Combined treatment with VPA and estrogen reduces neurofibrillary tangles in the brain in an ovariectomized mouse model of Alzheimer's disease after 4 weeks of drug administration.
(A) Western blot showing tau-5 and PHF-1 expression among all groups. (B) Quantification of the significant decrease in PHF-1 expression seen in all treatment groups compared with the control group. No difference was observed in tau-5 expression level among all groups. Relative protein expression was normalized to the control group. Data are presented as the mean ± SEM ($n = 8$). *$P < 0.05$, **$P < 0.01$, ***$P < 0.001$, ****$P < 0.0001$ (one-way analysis of variance followed by Tukey's *post hoc* test). E2: 17β-Estradiol; LG: liquiritigenin; PHF-1: paired helical filament-1; VPA: valproic acid.
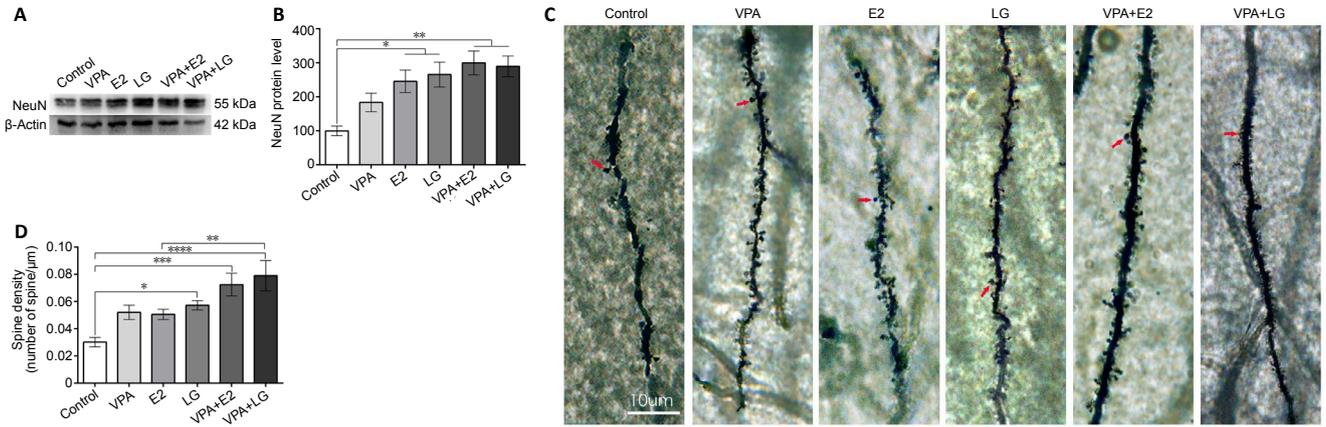
Figure 5 | Combined treatment with VPA and estrogen attenuates neuronal loss in an ovariectomized mouse model of Alzheimer's disease after 4 weeks of drug administration.
(A) Western blot showing NeuN expression among all groups. (B) NeuN was expressed at higher levels in all treatment groups, except the VPA-only group, compared with the control group. Relative protein expression was normalized to the control group. (C) Golgi staining showed that the dendritic spine density was increased in the LG and combined treatment groups compared with the control group. Scale bar: 10 μm. (D) Quantification of the increase in dendritic spine density seen in the LG and combination groups compared with the control group, as detected by Golgi staining. Data are presented as the mean ± SEM (n = 8). *P < 0.05, **P < 0.01, ***P < 0.001, ****P < 0.0001 (one-way analysis of variance followed by Tukey's *post hoc* test). E2: 17β-Estradiol; LG: liquiritigenin; NeuN: neuronal nuclei antigen; VPA: valproic acid.
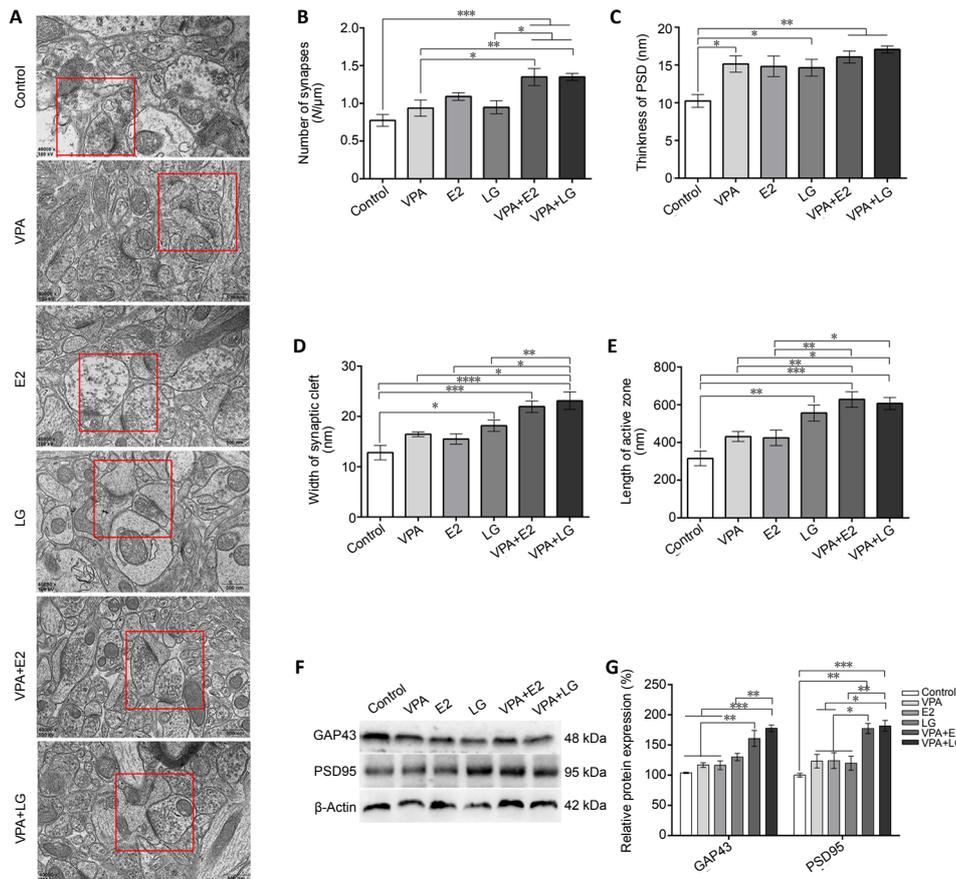

Figure 6 | Effect of combined treatment with VPA and estrogen on synapses in the brain in an ovariectomized mouse model of Alzheimer's disease after 4 weeks of drug administration.
(A) Transmission electron microscope images of brain sections. Synapses are shown in the red boxes. The number of synapse in the CA1 region of hippocampus was higher in the combined treatment groups compared with the control and single-drug groups. Scale bars: 500 nm. (B–D) Quantitative analysis of synapse structure. (B) The number of synapses in the hippocampus was higher in the combined treatment group than in the control and single-drug groups. (C) The PSD layer was significantly thicker in all of the treatment groups, except the E2 group, compared with the control group. (D, E) The synaptic cleft width (D) and synaptic active zone length (E) were greater in the LG and combined treatment groups compared with the control group. (F) Western blot showing GAP43 and PSD-95 levels in the single-drug groups, the combined treatment groups, and the control group. (G) Quantification of the striking increase in GAP43 and PSD-95 levels. Relative protein expression was normalized to the control group. Data are presented as the mean ± SEM (n = 8). *P < 0.05, **P < 0.01, ***P < 0.001, ****P < 0.0001 (one-way analysis of variance followed by Tukey's *post hoc* test). E2: 17β-Estradiol; GAP43: growth associated protein-43; LG: liquiritigenin; PSD95: postsynaptic density-95; VPA: valproic acid.

Discussion

VPA can reduce Aβ generation and SP formation by inhibiting GSK-3β-mediated β-secretase cleavage of APP, decrease tau hyperphosphorylation through GSK-3β signaling, and improve memory deficits in AD mice (Chen et al., 2018; Das et al., 2019). Interestingly, we previously found that the protective effects of VPA are greater in male AD mice than in female AD mice due low estrogen levels in the brains of the female mice. Estrogen can reduce Aβ production and tau hyperphosphorylation in the brain (Brann et al., 2007). However, women with advanced menopausal AD suffer from altered ERα and ERβ expression in the brain, resulting in an ERα/ERβ ratio imbalance, which dramatically reduces sensitivity to estrogen and renders estrogen replacement therapy treatment largely ineffective.

In this study, we found that treatment with VPA and estrogen is more effective than treatment with estrogen intervention alone, and can significantly improve spatial memory and learning in OVX AD mice. The progressive cognitive impairment seen in AD is closely correlated with neural plasticity exhaustion and synaptic loss (de Calignon et al., 2010; D'Amelio et al., 2011), which are early events in AD development (Scheff et al., 2007). Modification of synaptic connectivity correlates with a change in synapse
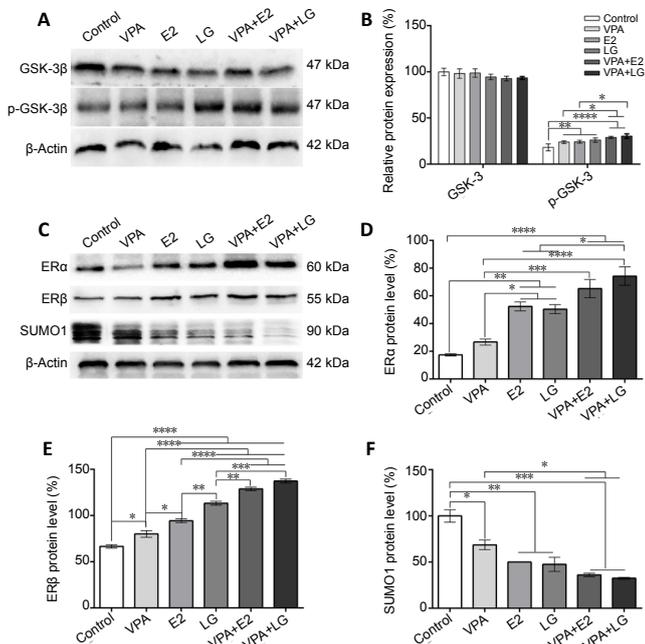
Figure 7 | Combined treatment with VPA and estrogen up-regulated GSK-3β expression in the brain in an ovariectomized mouse model of Alzheimer's disease after 4 weeks of drug administration.
(A) Western blot showing GSK-3β and p-GSK-3β expression among all groups. (B) Quantification of the significant increase in p-GSK-3β expression in the single-drug and combined treatment groups compared with the control group. There were no significant differences in t-GSK-3β expression among the groups. (C) Western blot showing ERα, ERβ, and SUMO1 expression among all groups. (D) Quantification of the increase in ERα expression in all of the single drug-groups except the VPA group, and the significant increase in ERα expression in the combined treatment groups compared with the control group. (E) Quantification of the significant increase in ERβ expression in all of the treatment groups, except the VPA-only group, compared with the control group. (F) Quantification of the significant decreased in SUMO1 expression in all treatment groups compared with the control group. Relative protein expression was normalized to the control group. Data are presented as the mean ± SEM (n = 8). *$P < 0.05$, **$P < 0.01$, ***$P < 0.001$, ****$P < 0.0001$ (one-way analysis of variance followed by Tukey's *post hoc* test). E2: 17β-estradiol; ER: estrogen receptor; GSK-3β: glycogen synthase kinase 3β; LG: liquiritigenin; SUMO1: small ubiquitin-like modifier 1; VPA: valproic acid.

number and density, which causes cognitive deficits and neural system dysfunction (Citri and Malenka, 2008). Here, TEM analysis revealed that the thickness of the PSD layer was increased when mice were treated with VPA and estrogen compared with the control group. PSD, which is an electron-dense material that is uniformly distributed across the postsynaptic membrane, plays important roles in postsynaptic signaling transduction and assembly (de Bartolomeis et al., 2014). Combined treatment with VPA and estrogen not only significantly increased the number and density of presynaptic vesicles, but led to upregulation of GAP-43 and PSD-95 (the synaptic protein markers), which are distributed on pre- and post-synaptic membranes and play a role in axonal regeneration and synaptic remodeling. Thus, treatment with VPA plus estrogen resulted in striking rescue of early synaptic impairment in OVX AD mice.

Aβ is generated from APP by a sequential limited proteolytic process mediated by β- and γ-secretases. This process is regulated by various enzymes, among which BACE1 and PS1 are the key enzymes involved in Aβ production, and IDE and NEP are the two main proteases responsible for Aβ degradation. Under normal circumstances, Aβ is constantly produced from its precursor and immediately catabolized (Selkoe and Hardy, 2016). When the balance of Aβ production and clearance is disrupted, Aβ accumulates in the brain. The results from our study show that the combined use of VPA and estrogen reduces BACE1 and PS1 levels in the brain of OVX AD mice and significantly up-regulates IDE and NEP expression, indicating that the combined treatment regimen can reduce

SP formation. Tau, a predominantly axonal microtubule-associated protein, promotes microtubule formation and maintains microtubule stability. Hyperphosphorylated tau is the principal component of neurofibrillary tangles, which interfere with normal neuronal function and eventually lead to neuronal degeneration and death (Avila et al., 2004). We found no difference in Tau-5 expression among the groups tested in this study; however, expression of PHF-1, which targets pSer396/pSer404 (Neddens et al., 2018), was significantly reduced in the brains of mice in all of the treatment groups, indicating that both VPA and estrogen can reduce tau hyperphosphorylation.

In this study, we investigated the effect and possible mechanisms of VPA combined with estrogen treatment in OVX AD mice. GSK-3β is major kinase associated with tau hyperphosphorylation and Aβ generation. GSK-3β inhibitors (lithium and tideglusib) failed to show significant cognitive or clinical benefits in AD patients in controlled trials (Matsunaga et al., 2019). However, other studies suggest that GSK-3β inhibitors might be beneficial for AD therapy (Maqbool et al., 2016; Saraswati et al., 2018; Jaworski et al., 2019). GSK-3β can affect ERα phosphorylation, thereby regulating its expression and activity (Medunjanin et al., 2005; Fortunati et al., 2010). In the present study we found that that the covalent binding of ERβ and SUMO1 can significantly inhibit ERβ transcriptional activity and its response to estrogen (Picard et al., 2012). SUMO is closely related to the progression of AD (Takahashi et al., 2008). For example, SUMO1 binding to AD-related proteins (e.g., tau, APP, and BACE1) (Dorval and Fraser, 2006; Zhang and Sarge, 2008; Yun et al., 2013) promotes Aβ production. Furthermore, ERβ binding to SUMO1 is regulated by GSK-3β: GSK-3β overexpression increases ERβ-SUMO1 expression, and decreased GSK-3β expression reduces ERβ-SUMO1 expression (Picard et al., 2012). We found no difference in GSK-3β levels among all of the groups tested, but did observe a significant increase in p-GSK-3β (ser9) content in all groups, especially in the group that was treated with both VPA and estrogen; phosphorylation of the GSK-3β ser9 residue inhibits its catalytic activity (Azab et al., 2017). In addition, SUMO1 expression was significantly reduced, and ERα and ERβ levels were markedly higher, in the combined group compared with the control group.

In summary, the current study confirms that VPA combined with estrogen is better than VPA or estrogen intervention alone in treating AD in a late menopausal mouse model. Although combining E2 or LG with VPA achieved similar results in terms of attenuating neuropathological features, the VPA + LG group demonstrated superior improvements in spatial memory and learning compared with the VPA + E2 group. VPA could enhance ER sensitivity to estrogen by inhibiting GSK-3β activity, consequently improving spatial memory and learning, reducing Aβ deposition and tau hyperphosphorylation, promoting neuronal maturation, and improving synaptic structure and function. However, more *in vitro* and *in vivo* studies are needed to identify the interactions between and regulatory mechanisms of GSK-3β and ERs in AD.

References

Avila J, Lucas JJ, Perez M, Hernandez F (2004) Role of tau protein in both physiological and pathological conditions. Physiol Rev 84:361-384.

Azab AN, Vainer E, Agam G, Bersudsky Y (2017) Lymphocyte phospho-Ser-9-GSK-3β/total GSK-3β protein levels ratio is not affected by chronic lithium or valproate treatment in euthymic patients with bipolar disorder. J Clin Psychopharmacol 37:226-230.

Brann DW, Dhandapani K, Wakade C, Mahesh VB, Khan MM (2007) Neurotrophic and neuroprotective actions of estrogen: basic mechanisms and clinical implications. Steroids 72:381-405.

Chen JY, Chu LW, Cheng KI, Hsieh SL, Juan YS, Wu BN (2018) Valproate reduces neuroinflammation and neuronal death in a rat chronic constriction injury model. Sci Rep 8:16457.

Chidambaram SB, Rathipriya AG, Bolla SR, Bhat A, Ray B, Mahalakshmi AM, Manivasagam T, Thenmozhi AJ, Essa MM, Guillemin GJ, Chandra R, Sakharkar MK (2019) Dendritic spines: Revisiting the physiological role. Prog Neuropsychopharmacol Biol Psychiatry 92:161-193.

Citri A, Malenka RC (2008) Synaptic plasticity: multiple forms, functions, and mechanisms. Neuropsychopharmacology 33:18-41.

D'Amelio M, Cavallucci V, Middei S, Marchetti C, Pacioni S, Ferri A, Diamantini A, De Zio D, Carrara P, Battistini L, Moreno S, Bacci A, Ammassari-Teule M, Marie H, Cecconi F (2011) Caspase-3 triggers early synaptic dysfunction in a mouse model of Alzheimer's disease. Nat Neurosci 14:69-76.

Das TK, Jana P, Chakrabarti SK, Abdul Hamid MRW (2019) Curcumin downregulates GSK3 and Cdk5 in scopolamine-induced Alzheimer's disease rats abrogating Aβ(40/42) and tau hyperphosphorylation. J Alzheimers Dis Rep 3:257-267.

de Bartolomeis A, Latte G, Tomasetti C, Iasevoli F (2014) Glutamatergic postsynaptic density protein dysfunctions in synaptic plasticity and dendritic spines morphology: relevance to schizophrenia and other behavioral disorders pathophysiology, and implications for novel therapeutic approaches. Mol Neurobiol 49:484-511.

de Calignon A, Fox LM, Pitstick R, Carlson GA, Bacskai BJ, Spires-Jones TL, Hyman BT (2010) Caspase activation precedes and leads to tangles. Nature 464:1201-1204.

Dorval V, Fraser PE (2006) Small ubiquitin-like modifier (SUMO) modification of natively unfolded proteins tau and alpha-synuclein. J Biol Chem 281:9919-9924.

Fortunati N, Bertino S, Costantino L, De Bortoli M, Compagnone A, Bandino A, Catalano MG, Boccuzzi G (2010) Valproic acid restores ER alpha and antiestrogen sensitivity to ER alpha-negative breast cancer cells. Mol Cell Endocrinol 314:17-22.

Foster TC (2012) Role of estrogen receptor alpha and beta expression and signaling on cognitive function during aging. Hippocampus 22:656-669.

Gillies GE, McArthur S (2010) Estrogen actions in the brain and the basis for differential action in men and women: a case for sex-specific medicines. Pharmacol Rev 62:155-198.

Gleason CE, Dowling NM, Wharton W, Manson JE, Miller VM, Atwood CS, Brinton EA, Cedars MI, Lobo RA, Merriam GR, Neal-Perry G, Santoro NF, Taylor HS, Black DM, Budoff MJ, Hodis HN, Naftolin F, Harman SM, Asthana S (2015) Effects of hormone therapy on cognition and mood in recently postmenopausal women: Findings from the randomized, controlled KEEPS-cognitive and affective study. PLoS Med 12:e1001833; discussion e1001833.

Goedert M, Spillantini MG (2006) A century of Alzheimer's disease. Science 314:777-781.

He LX, Wan L, Xiang W, Li JM, Pan AH, Lu DH (2020) Synaptic development of layer V pyramidal neurons in the prenatal human prefrontal neocortex: a Neurolucida-aided Golgi study. Neural Regen Res 15:1490-1495.

Hernández F, Gómez de Barreda E, Fuster-Matanzo A, Lucas JJ, Avila J (2010) GSK3: a possible link between beta amyloid peptide and tau protein. Exp Neurol 223:322-325.

Hu JP, Xie JW, Wang CY, Wang T, Wang X, Wang SL, Teng WP, Wang ZY (2011) Valproate reduces tau phosphorylation via cyclin-dependent kinase 5 and glycogen synthase kinase 3 signaling pathways. Brain Res Bull 85:194-200.

Jaworski T, Banach-Kasper E, Gralec K (2019) GSK-3β at the intersection of neuronal plasticity and neurodegeneration. Neural Plast 2019:4209475.

Kantarci K, Lowe VJ, Lesnick TG, Tosakulwong N, Bailey KR, Fields JA, Shuster LT, Zuk SM, Senjem ML, Mielke MM, Gleason C, Jack CR, Rocca WA, Miller VM (2016) Early postmenopausal transdermal 17β-estradiol therapy and amyloid-β deposition. J Alzheimers Dis 53:547-556.

Kostrouchová M, Kostrouch Z, Kostrouchová M (2007) Valproic acid, a molecular lead to multiple regulatory pathways. Folia Biol (Praha) 53:37-49.

Lorenz B, Garcia-Segura LM, DonCarlos LL (2005) Cellular phenotype of androgen receptor-immunoreactive nuclei in the developing and adult rat brain. J Comp Neurol 492:456-468.

Lyu D, Tang N, Womack AW, He YJ, Lin Q (2020) Neonatal ketamine exposure-induced hippocampal neuroapoptosis in the developing brain impairs adult spatial learning ability. Neural Regen Res 15:880-886.

Maqbool M, Mobashir M, Hoda N (2016) Pivotal role of glycogen synthase kinase-3: A therapeutic target for Alzheimer's disease. Eur J Med Chem 107:63-81.

Matsunaga S, Fujishiro H, Takechi H (2019) Efficacy and safety of glycogen synthase kinase 3 inhibitors for Alzheimer's disease: A systematic review and meta-analysis. J Alzheimers Dis 69:1031-1039.

Medunjanin S, Hermani A, De Servi B, Grisouard J, Rincke G, Mayer D (2005) Glycogen synthase kinase-3 interacts with and phosphorylates estrogen receptor alpha and is involved in the regulation of receptor activity. J Biol Chem 280:33006-33014.

Mersereau JE, Levy N, Staub RE, Baggett S, Zogovic T, Chow S, Ricke WA, Tagliaferri M, Cohen I, Bjeldanes LF, Leitman DC (2008) Liquiritigenin is a plant-derived highly selective estrogen receptor beta agonist. Mol Cell Endocrinol 283:49-57.

Murphy MP, LeVine H, 3rd (2010) Alzheimer's disease and the amyloid-beta peptide. J Alzheimers Dis 19:311-323.

Neddens J, Temmel M, Flunkert S, Kerschbaumer B, Hoeller C, Loeffler T, Niederkofler V, Daum G, Attems J, Hutter-Paier B (2018) Phosphorylation of different tau sites during progression of Alzheimer's disease. Acta Neuropathol Commun 6:52.

Picard N, Caron V, Bilodeau S, Sanchez M, Mascle X, Aubry M, Tremblay A (2012) Identification of estrogen receptor β as a SUMO-1 target reveals a novel phosphorylated sumoylation motif and regulation by glycogen synthase kinase 3β. Mol Cell Biol 32:2709-2721.

Qing H, He G, Ly PT, Fox CJ, Staufenbiel M, Cai F, Zhang Z, Wei S, Sun X, Chen CH, Zhou W, Wang K, Song W (2008) Valproic acid inhibits Abeta production, neuritic plaque formation, and behavioral deficits in Alzheimer's disease mouse models. J Exp Med 205:2781-2789.

Saraswati AP, Ali Hussaini SM, Krishna NH, Babu BN, Kamal A (2018) Glycogen synthase kinase-3 and its inhibitors: Potential target for various therapeutic conditions. Eur J Med Chem 144:843-858.

Scheff SW, Price DA, Schmitt FA, DeKosky ST, Mufson EJ (2007) Synaptic alterations in CA1 in mild Alzheimer disease and mild cognitive impairment. Neurology 68:1501-1508.

Selkoe DJ, Hardy J (2016) The amyloid hypothesis of Alzheimer's disease at 25 years. EMBO Mol Med 8:595-608.

Šimić G, Babić Leko M, Wray S, Harrington C, Delalle I, Jovanov-Milošević N, Bažadona D, Buée L, de Silva R, Di Giovanni G, Wischik C, Hof PR (2016) Tau protein hyperphosphorylation and aggregation in Alzheimer's disease and other tauopathies, and possible neuroprotective strategies. Biomolecules 6:6.

Sinopoli KJ, Floresco SB, Galea LA (2006) Systemic and local administration of estradiol into the prefrontal cortex or hippocampus differentially alters working memory. Neurobiol Learn Mem 86:293-304.

Spires-Jones TL, Hyman BT (2014) The intersection of amyloid beta and tau at synapses in Alzheimer's disease. Neuron 82:756-771.

Takahashi K, Ishida M, Komano H, Takahashi H (2008) SUMO-1 immunoreactivity co-localizes with phospho-Tau in APP transgenic mice but not in mutant Tau transgenic mice. Neurosci Lett 441:90-93.

Vasic V, Barth K, Schmidt MHH (2019) Neurodegeneration and neuro-regeneration-Alzheimer's disease and stem cell therapy. Int J Mol Sci 20:4272.

Wang JC, Liu HY, Cao YP (2020) tau protein and Alzheimer's disease. Zhongguo Zuzhi Gongcheng Yanjiu 24:2775-2781.

Xuan AG, Pan XB, Wei P, Ji WD, Zhang WJ, Liu JH, Hong LP, Chen WL, Long DH (2015) Valproic acid alleviates memory deficits and attenuates amyloid-β deposition in transgenic mouse model of Alzheimer's disease. Mol Neurobiol 51:300-312.

Yun SM, Cho SJ, Song JC, Song SY, Jo SA, Jo C, Yoon K, Tanzi RE, Choi EJ, Koh YH (2013) SUMO1 modulates Aβ generation via BACE1 accumulation. Neurobiol Aging 34:650-662.

Zhang YQ, Sarge KD (2008) Sumoylation of amyloid precursor protein negatively regulates Abeta aggregate levels. Biochem Biophys Res Commun 374:673-678.